Homologous recombination deficiency and tumor suppressor heterozygosity mediate resistance to front-line therapy in breast cancer

Anton Safonov[1,2], Antonio Marra[3], Chaitanya Bandlamudi[4], Ben O'Leary[5], Bradley Wubbenhorst[6], Enrico Moiso[1,4], Minna Lee[7,8], Mark T.A. Donoghue[7], Julia An[9], Marie Will[1,10], Fresia Pareja[11], Mehnaj Ahmed[1,9], Emily Nizialek[12], Natalia Lukashchuk[12], Eleni Sofianopoulou[12], Yuan Liu[13], Xin Huang[13], Nikolaus Schultz[4], Michael Berger[4,11], Maurizio Scaltriti[12], Jorge S. Reis-Filho[12], Bob T. Li[1,9], Ken Offit[10], Larry Norton[1], David B. Solit[1,8], Sohrab Shah[4], Kara N. Maxwell[6], Susan M. Domchek[6], Fergus Couch[14], Katherine L. Nathanson[6], Mark E. Robson[1,2,10], Nicholas C. Turner[5], Sarat Chandarlapaty[1,2,8], Pedram Razavi[1,2,9]

Affiliations

[1] Department of Medicine, Memorial Sloan Kettering Cancer Center, New York, United States

[2] Weill Cornell Medical College, New York, United States

[3] IEO, Istituto Europeo di Oncologia, IRCCS, Milan, Italy.

[4] Computational Oncology Service, Memorial Sloan Kettering Cancer Center, New York, United States

[5] Royal Marsden Hospital and Institute of Cancer Research, London, United Kingdom

[6] Abramson Cancer Center, University of Pennsylvania, Philadelphia, United States

[7] Department of Surgery, Memorial Sloan Kettering Cancer Center, New York, United States

[8] Human Oncology and Pathogenesis Program, Memorial Sloan Kettering Cancer Center, New York, United States

[9] Global Biomarker Development Program, Memorial Sloan Kettering Cancer Center, New York, United States

[10] Clinical Genetics Service, Memorial Sloan Kettering Cancer Center, New York, United States

[11] Department of Pathology, Memorial Sloan Kettering Cancer Center, New York, United States

[12] AstraZeneca, Cambridge, United Kingdom

[13] Pfizer, New York, United States

[14] Experimental Pathology and Laboratory Medicine, Mayo Clinic, Rochester, Minnesota, United States

Correspondence: Pedram Razavi, razavip@mskcc.org

Abstract:

Germline and somatic variants that drive breast tumorigenesis and therapeutic sensitivity are widely prevalent. The clinical and biologic significance of co-occurring disease-defining germline and somatic events have yet to be defined and exploited. Using multiple, independent clinical cohorts comprising over 4500 patients, we identify that pathogenic *RB1* variants are enriched in g*BRCA2*-associated cancers, and manifest poor outcomes on standard-of-care front-line CDK4/6i plus antiestrogen combinations. We demonstrate g*BRCA2*-associated cancers commonly give rise to allelic configurations manifesting *RB1* heterozygosity and readily lose the second copy through *gBRCA2* loss-mediated homologous recombination deficiency (HRD) under the therapeutic pressure of CDK4/6i. The findings unveil a novel therapeutic strategy of targeting the underlying HRD through PARPi *prior to* CDK4/6i to intercept the deleterious *RB1*-loss trajectory. The work reveals how germline-somatic driven genomic configurations can shape treatment responses and be exploited in biomarker-directed clinical strategies.

INTRODUCTION

Inherited pathogenic variants (PVs) in cancer susceptibility genes predispose to tumor development[1,2]. Characteristically, these genes play fundamental roles in DNA damage repair [3–6] or cell cycle pathways[7–9]. Recent technological advances have ushered in a rapid adoption of more expansive germline genetic testing to identify PVs. In parallel, the identification of *somatic* alterations affecting commonly implicated oncogenic pathways serves as a central tenet of precision oncology[10].

Recent studies integrating germline and somatic features have explored the concept that landscapes of somatic variants may be shaped by the pre-existing germline features of a tumor [11–16]. However, these largely pan-cancer studies have not comprehensively incorporated biologically relevant subtypes (e.g. receptor status in breast cancer). Additionally, the clinical implications of such germline-somatic interactions have not been explored; this is an avenue of significant relevance as clinical treatments can be guided from both categories of variants. Targeted therapies are readily available to exploit aforementioned patterns of DNA disrepair stemming from *germline* alterations, such as PARP inhibitors (PARPi) in homologous recombination (HRD)-driven tumors[17,18]. Somatic variants, on the other hand, not only serve as actionable targets themselves, but also have been extensively implicated as mechanisms of resistance to various targeted therapy strategies[19].

An abundance of choice between approved germline, somatic, and lineage-directed therapy often leads to ambiguity in selecting the optimal sequencing of therapies. This immediate clinical dilemma is exemplified in the management of g*BRCA2*-driven breast cancers, the majority of

which demonstrate estrogen receptor overexpression (ER+)[20]. The combination of CDK4/6 inhibitors (CDK4/6i) and endocrine therapy (ET) therefore serves as standard-of-care front-line treatment strategy in both the metastatic and adjuvant treatment setting[21–23], but it is unclear whether this strategy should be deployed prior to PARPi, which are approved and effective alternative treatment options in both adjuvant and metastatic settings. Specifically, little is known about whether the somatic variants evident in g*BRCA2* confer response or resistance to these standard-of-care front line therapies. On a more general level, defining the role of pre-treatment germline and somatic genomic context on evolutionary trajectories of *acquired* treatment resistance would be an invaluable contribution to the precision oncology arsenal.

To elucidate the relevance of the underlying germline process to the somatic genotype in a clinically relevant context, we performed an integrated analysis of germline and somatic next generation sequencing data, paired with expertly annotated clinical data. Through statistical analysis of a large institutional clinicogenomic cohort and external validation from manifold multi-institutional resources, we demonstrated that g*BRCA2* PVs indeed results in poor outcomes to standard of care first line CDK4/6i and ET. We further determined the mechanisms underlying this phenotype including facilitated acquisition of *RB1* loss-of-function variants stemming from HRD-driven mutagenesis and vulnerable pre-treatment somatic *RB1* allelic pattern heralding complete Rb1 loss. Lastly, we expand the latter point to define pre-treatment somatic allelic configuration as an identifiable predictor of acquired “second hit” somatic variants.

MAIN

Clinicopathological and genomic features of germline HRD-related variants

To identify the interactions between germline and somatic oncogenic variants in breast cancer, we analyzed prospectively collected sequencing data from 4,640 patients with a diagnosis of breast cancer. Germline blood and matched tumor tissue DNA was sequenced using an FDA authorized clinical sequencing assay encompassing up to 468 cancer-associated genes, including germline analysis of 84 well-established cancer predisposition genes[24–26]. Particular genes of interest for the germline analysis included canonical members in the homologous recombination pathway: *BRCA2* (pathogenic variants in 127 patients; 28% of cohort), *BRCA1* (n = 105, 2.4%), *CHEK2* (n = 97, 2.2%), *ATM* (n = 45, 1.0%), *PALB2* (n = 25, 0.6%).

The clinicopathologic characteristics of the germline-altered cancers and germline WT cancers strongly reflected previously established patterns suggesting that our cohort was representative of general population of patients with breast cancer (**Table 1**). Specifically, we observed a younger age of diagnosis with g*BRCA1*, g*BRCA2*, or g*CHEK2* compared to *gWT* (wild-type) cases, while our cohort was likely underpowered to detect such differences in carriers of g*ATM* or g*PALB2.* As expected, g*BRCA1*-associated breast cancers tended to be triple-negative[27,28], high grade invasive ductal carcinoma. g*BRCA2* and g*CHEK2* (71.0%, 74.6%, respectively) tended to result in HR+/HER2- disease, consistent with prior studies[29,30].

Furthermore, genomic analysis of our cohort confirmed prior gene-specific zygosity trends. Loss of heterozygosity (LOH), or loss of wild-type allele is often necessary for phenotypic impact in carriers of germline pathogenic variants in HRD-related genes. It has been previously suggested

that the incidence of biallelic alterations is gene dependent[31,32]. Our results confirmed that the rate of biallelic inactivation varied widely among our genes of interest in evaluable cases, ranging from 47.5% in g*CHEK2,* to 88.8% and 89.7% in g*BRCA1* and g*BRCA2,* respectively. Similarly, we recapitulate prior evidence describing the relatively lower frequency of LOH in g*PALB2* carriers (n = 12, 60.0%), but a relatively higher frequency of "second-hit" somatic mutations resulting in biallelic loss (n = 4, 20.0%)[33]. Taken together, these results establish the histological, demographic and genomic features associated with germline PVs in a large cohort of patients with early-stage and advanced breast cancer.

Germline-somatic interaction analysis uncover clinical actionability

We sought to define patterns of mutual exclusivity or enrichment of somatic variants with each germline pathogenic variant of interest (hereafter referred to as germline-somatic interactions), in the context of receptor status and zygosity. We compiled mutations, fusions, copy number alterations predicted to be functionally significant utilizing OncoKB[34], and performed enrichment analyses (**Fig. 1a)**.

Germline-somatic analysis of our cohort robustly confirmed previously established relationships such as the enrichment of *TP53* somatic alterations seen in *gBRCA1* carriers and mutual exclusivity of *gATM* and *TP53* alterations (**Fig. 1b,c**). Both findings were more pronounced when analysis was limited to tumors exhibiting biallelic inactivation of the respective genes, supporting the aforementioned causative link between biallelic loss of an HRD-related gene and a particular phenotypic sequelae [32,35](**Fig. S3**). We furthered these observations by conducting receptor status-dependent explorations of germline-somatic interactions. For instance, the

gBRCA1:*TP53* enrichment was prominent in HR+/HER2- cases as well as triple-negative cases (**Fig. S3**). These data support the assertion that *TP53* loss-of-function is a fundamental event in the oncogenesis of a *gBRCA1*-driven tumor [36–38], rather than confounded by the enrichment of triple negative breast cancers seen in *gBRCA1* mutated cases.

Strikingly, g*BRCA2*-driven breast cancers harbor several somatic alterations of immediate clinical interest. *RB1* somatic variants represent the most significant enrichment in tumors with g*BRCA2* pathogenic variants (**Fig. 1d**). This was in contrast to g*BRCA1* where *RB1* somatic variants were relatively depleted (**Fig. 1c**). Limiting the analysis to HR+/HER2- cases (71.0% of *gBRCA2*) results in even more apparent enrichment of somatic *RB1* alterations in g*BRCA2.* Additionally, this analysis uncovered an enrichment of *MYC* and *AURKA* amplifications in this context. Both of these alterations have also been implicated in CDK4/6i resistance[39–41]. Conversely, *PIK3CA* alterations trend towards mutual exclusivity in both *gBRCA2* and g*BRCA1*-driven samples. **Fig. 1e** displays the somatic variant type and pathologic features of g*BRCA2*-associated samples.

Germline *BRCA2* driven breast cancers exhibit resistance to standard frontline therapy

RB1 loss is an established mechanism of resistance to CDK4/6i inhibitors[42]. Based on our enrichment results demonstrating a significant enrichment of *RB1* alterations in g*BRCA2*, we analyzed the impact of g*BRCA2* status on progression free survival on CDK4/6i and ET. In the first line setting, 537 patients were evaluable for outcomes on CDK4/6i, while 1103 patients were evaluable for treatment with CDK4/6i in any treatment line. Germline *BRCA2* status was associated with a significantly worse progression free survival (PFS) on CDK4/6i and ET in the

univariate and multivariate settings (median PFS 8.7 vs 13.0 months, Hazard Ratio [HR] 2.22, 95% CI 1.50 – 3.27, $p < 0.0001$) (**Fig. 2a).** Similar results were seen when the analysis was extended to all treatment lines, with consideration of endocrine therapy partner and treatment line as covariates (HR 2.04 95% CI 1.53 – 2.70, $p < 0.0001$) (**Fig. 2b).**

We next aimed to evaluate the findings with an independent dataset from HR+/HER2- metastatic breast cancer patients treated with 1st line CDK4/6i and ET. We employed the Flatiron Health database, a nationwide clinicogenomic dataset containing patient-level outcomes data from a combination of community oncology settings and academic medical centers[43]. Our analysis based on 2185 patients (62 with g*BRCA2*) confirmed our findings with a strong association between g*BRCA2* and poor PFS on CDK4/6i (HR 1.82, 95% CI 1.35-3.45, $p< 0.0001$) (**Fig. 2c).**

In a subgroup of patients who received a subsequent line of a PARPi after progression on CDK4/6i (n = 35), we observed that this HRD-directed therapy resulted in generally superior outcomes (**Fig. 2d)**. The widely expected result for therapies is that later lines of therapy would result in relatively shorter progression free survival (PFS). PFS on PARPi exceeded PFS of CDK4/6i and ET. Of the 34 patients who did not experience a toxicity event from either PARPi or CDK4/6i, only fourteen (41.2%) had a partial or complete response to CDK4/6i and ET, while twenty-seven (79.4%) had partial or complete response to subsequent-line PARPi. In this g*BRCA2* dataset, there was a statistically significant enrichment for cases which responded to PARPi after no measured response to prior CDK4/6i and ET. Representative cases of rapid progression through first line CDK4/6i and endocrine therapy, followed by prolonged complete metabolic response to PARPi are outlined in **Figures 2e,f**. These results provide rationale for

prioritization of PARPi in this group of patients with expected poor outcomes on CDK4/6i. Taken together, these results represent the first robust example of a particular germline alteration predicting resistance to standard of care targeted therapies in breast cancer.

Clinicogenomic analysis suggests evolutionary acquisition of *RB1*

To investigate potential mechanisms underlying g*BRCA2*:*RB1* co-alterations, we evaluated the clinicopathologic context of somatic *RB1* function mutations. Intriguingly, while somatic *RB1* variants are mostly found in triple negative breast cancers in the g*WT* setting, the majority of g*BRCA2*:*RB1* co-alterations occur in HR+/HER2- disease. (**Fig. 3a).** Somatic *RB1* loss-of-function variants were also significantly enriched in the metastatic samples as compared to treatment-naive primaries, suggesting that *RB1* loss occurs during a more advanced stage in tumor evolution, rather than as a founding tumorigenesis event. This trend was especially notable in the g*BRCA2* samples, with 80% of *RB1* loss variants occurring in samples which have been exposed to systemic treatment.

To further investigate the implications of germline status on development of *RB1* loss, we assembled a large cohort of patients with paired pre- and post-CDK4/6i sequenced tumors (n=346 tumors from 173 patients). Indeed, our analysis demonstrated that acquisition of somatic *RB1* loss-of-function events was significantly more prevalent in *gBRCA2*-associated tumors vs g*BRCA2* WT tumors (35.3% vs 7.4%, OR 7.79, 95% CI 2.23 – 28.3, p = 0.0016) (**Fig. 3b).** While formal mutual exclusivity analysis in this setting was underpowered, we did not observe an overlap between acquisition of *RB1* and the presence or acquisition of any other established genomic CDK4/6i resistance mechanism.

This specific connection is further depicted in two representative g*BRCA2* HR+/HER2- metastatic breast cancer patients (**Figs. 3c,d**), wherein the patients experienced a short PFS on CDK4/6i and ET, followed by a more pronounced and durable response to PARPi. Remarkably, acquired polyclonal *RB1* loss of function variants were seen in both cases in post-CDK4/6i setting. The convergent evolution under the selective pressure of CDK4/6i resulting in the same mechanism of resistance in different clones serves as evidence of strong and specific evolutionary pressure for *RB1* loss-of-function in these g*BRCA2* tumors.

Inherent copy number structure of *BRCA2*-driven tumors facilitates on-treatment *RB1* loss

Consideration of the genomic structure of *BRCA2*-driven tumors provides further insight into the specific enrichment of *RB1* loss in this context. These genes are both co-located on chromosome 13q, and previous work suggested that biallelic inactivation of *BRCA2* in g*BRCA2*-driven tumors often occurs through LOH as a result of loss of a large chromosomal segment including the WT allele[44,45]. To confirm this finding, we analyzed the data from our cohort, which demonstrated a clear co-occurrence of *BRCA2* and *RB1* LOH) in g*BRCA2* tumors (n = 61, 77.2% of evaluable cases; OR 8.70, 95% CI 5.01 – 15.81, $p < 0.0001$) (**Fig. 4a)**. Despite this clear enrichment in g*BRCA2* tumors, it is notable that *RB1* LOH is also observed in gWT cases as well (n = 495, 28.0% of evaluable cases). We sought to evaluate the incidence of this phenomenon on an external, multi-institutional cohort of g*BRCA2*-driven breast cancers. We performed Allele Specific Copy Number (ASCN) analysis on 22 g*BRCA2* cases from University of Pennsylvania Abramason Cancer Center and 22 g*BRCA2* cases from Mayo Clinic (n = 44 total) which were profiled with whole exome sequencing (WES). Out of these 44 cases, 39 (88.6%) demonstrated

LOH of *BRCA2* and 37 (84.1%) demonstrated concurrent LOH of *BRCA2* and *RB1*. This co-occurrence was statistically significant ($p < 0.0001$), and provides independent cohort validation of the findings (**Fig. S8**).

We hypothesized that *RB1* LOH could be the predominant reason behind CDK4/6i resistance in g*BRCA2* associated tumors featuring genomic instability in the form of HRD. In other cancers, alternative forms of genomic instability may also promote CDK4/6i resistance through RB1 LOH. Hence, we extended our survival analyses to consider whether pre-treatment *RB1* zygosity may predict outcome on CDK4/6i therapy beyond the context of g*BRCA2* status. We considered patients in our institutional cohort who underwent somatic profiling of tumors obtained prior to start of 1st line CDK4/6i therapy from which LOH status was evaluable (n = 365 patients). *RB1* LOH was observed in 48.7% of these patients, and portended both significantly shorter PFS (HR 2.0, 95% CI 1.6 – 2.5, $p < 0.0001$) as well as worse overall survival (OS, HR 1.4, 95% CI 1.0 – 1.8, $p = 0.027$, **Figs. 4b-c)**.

We sought to confirm these findings in an independent cohort. The PALOMA-3 study was the pivotal phase III trial of palbociclib and fulvestrant vs fulvestrant alone in patients with metastatic HR+/HER2- breast cancer which had progressed on prior endocrine therapy which resulted in the regulatory approval of Palbociclib. Baseline circulating tumor DNA (ctDNA) from the fulvestrant and palbociclib combination arm was sequenced using a 1729 amplicon custom AmpliSeq panel, which included 119 SNPs within *RB1*. Circulating tumor DNA-based LOH analysis was conducted using a bespoke pipeline[46,47], yielding *RB1* LOH in 19 (7.3%) of 259 baseline ctDNA samples. *RB1* LOH was observed less frequently than our institutional

datasets due to fundamentally different methods of measurement between the two cohorts. LOH detection from ctDNA requires high amounts of circulating tumor DNA, therefore there is a decreased detection rate in PALOMA-3 compared to our solid tumor-derived MSK-IMPACT cohort. Consistent with our findings, *RB1* LOH in the PALOMA cohort conferred a significantly worse PFS (HR 2.2, 95% CI 1.3 – 3.8, p = 0.0044) as well as an inferior OS (HR 3.28, 95% CI 2.02 – 5.32, p < 0.0001) (**Fig. 4d,e)**.

Pre-treatment *RB1* allele-specific copy number profile predicts acquisition of *RB1* loss under therapeutic pressure of CDK4/6i

The definition of LOH employed thus far encompasses not only tumors with a single allele of *RB1* (heterozygous loss), but also LOH in more complex genomic backgrounds such as loss before or after whole genome duplication **(Fig. 4f).** To investigate the clinical relevance of heterozygous loss, as compared to other allelic states involving more than one remaining allele, we employed allele specific copy number analysis to assign more precise definitions to pre-treatment samples. Heterozygous loss was present in **(**30.9%, n = 112) of pre-treatment tumors, while (16.8%, n = 61) demonstrated evidence of other LOH. Both allelic configurations were associated with worse outcomes on CDK4/6i and ET (**Fig. 4g)**. As chromosomal instability and whole genome doubling are known to be poor prognostic factors in both the pan-cancer and breast cancer settings[48], we repeated the analysis with inclusion of fraction genome altered (FGA) as a covariate. Indeed, *RB1* het loss remained to be the sole significant allelic configuration in this multivariate analysis, while other *RB1* LOH patterns were no longer associated with poor PFS **(Fig. S9B).** Conversely, considering the overall survival analysis with refined allele-specific copy number assessments demonstrates that other allelic imbalances are

uniquely associated with a worse prognosis (HR 1.61, 95% CI 1.10 – 2.34, p = 0.01, **Fig. S9C).** These results indicate that the grouping of other allelic imbalance patterns in *RB1* represents a *prognostic* biomarker, while *RB1* het loss serves as a *predictive* biomarker of outcome to CDK4/6i therapy specifically.

To further explore the role of *RB1* allelic imbalance on CDK4/6i resistance, we extended our analysis of pre- and post- CDK4/6i tumors (n=173 patients) into these refined *RB1* allele-specific copy number definitions. Compared to *RB1* diploid status and other LOH states, pre-treatment *RB1* single allele status (het loss) uniquely predisposed to acquisition of *RB1* loss-of-function variant upon exposure to CDK4/6i (**Fig. 4h).** Notably, *RB1* loss-of-function alterations were observed more frequently in tumors with pre-treatment *RB1* het loss (19.2%) while such alterations were seldomly observed in any other setting (either existing pre-treatment or acquired post CDK4/6i from diploid and other LOH groups).

In our overall matched cohort acquired *RB1* loss developed in 15 (8.4%) of total post CDK4/6i samples, consistent with prior observations[46,49]. Although acquisition of *RB1* loss on CDK4/6i is relatively rare in an unselected population, our results demonstrate that *RB1* loss under the therapeutic pressure of CDK4/6i is observed almost exclusively in cancers who had only one functional allele of *RB1* pretreatment. This has major clinical implications for advanced surveillance strategies and patient selection for clinical trials of precision therapeutic strategies directed against complete *RB1* loss[50,51]. Most broadly, these results demonstrate how pre-treatment allelic structure of tumor suppressor genes may predict not only the therapeutic

outcome of a particular targeted therapy, but may also forecast the *specific* mechanism by which a desired therapy will ultimately fail.

HRD-driven mutagenesis facilitates acquisition of specific resistance mechanisms

Further analysis of our MSK cohort strongly suggested that *RB1* LOH configuration is only partially responsible for the exceptionally rapid progression seen with g*BRCA2*-driven tumors. *RB1* LOH confers shorter PFS in germline wild type cases (HR 1.89 95% CI 1.47 – 2.43, p = 6.91 e -7) compared to non-LOH *RB1* allelic configurations. However, *RB1* LOH in the context of *gBRCA2* a pathogenic variant portends an even worse prognosis (HR 2.73 95% CI 1.53 – 4.86, p = 0.00064) (**Fig. 4i).**

To determine whether gBRCA2 mediated HRD specifically contributes to the acquisition of somatic *RB1* loss-of-function variants, we analyzed the types of alterations in *RB1* found in our cohort. We observe a statistically significant enrichment for short indels and structural variants of *RB1* in the g*BRCA2* setting, indicative of *BRCA2*-deficiency mediated DNA disrepair (**Fig. 4j)**. The majority (75%, n=6) of post-CDK4/6i somatic *RB1* variants found in the g*BRCA2* tumors were short indels. Microhomology-mediated end joining (MMEJ) is a commonly implicated back-up DNA repair mechanism demonstrated in HRD-driven tumors[44,45], and can be identified by a characteristic pattern of microhomology flanking a short deletion. Indeed, 66% of short indels resulting in *RB1*-loss post-CDK4/6i were reflective of MMEJ.

Thus, these tumors appeared to exploit the imperfections of back-up DNA repair mechanisms present in *BRCA2*-driven tumors to escape therapeutic pressure. This phenomenon is similar to

the concept of "exaptation", which refers to an evolutionary co-option of a particular trait to serve a purpose distinct from the originally evolved role[52]. Similarly to *RB1* LOH*, HRD* status appears to confer worse outcomes to CDK4/6i when queried outside of the context of g*BRCA2* [**Fig S10**]. Our work strongly supports a dual mechanism to explain the particularly poor outcome and specific evolutionary trajectory in g*BRCA2*. Both an increased prevalence in *RB1* LOH and underlying HRD-driven mutagenesis to hasten the acquisition *RB1* loss-of-function mutations separately confer poor outcomes to CDK4/6i. Germline *BRCA2*-driven tumors harbor both features in unison, driving treatment failure to CDK4/6i.

DISCUSSION

We describe the largest known retrospective evidence that g*BRCA2* carriers experience shorter progression free survival on combination CDK4/6i plus ET, which is otherwise the standard of care frontline approach in the metastatic HR+/HER2- setting. Notably, we were able to validate our findings in independent large multi-institutional real-world data that was representative of general population of patients with metastatic breast cancer treated in community and academic settings. These data demonstrate that HRD states produce a permissive state for resistance acquisition, given the mutagenic nature of back-up DNA repair mechanisms coupled with the tendency of these tumors to have frequent patterns of heterozygous loss.

The mutagenesis conferred by HRD is itself subject to clinical intervention. Restoration of homologous recombination proficiency is an established mechanism of resistance to these PARPi. This phenomenon, taken in the context of our observations, bears significant implications for clinical practice. Presently, both CDK4/6i-based therapy and PARPi are noted in

the guideliens as the initial treatment modality for metastatic HR+/HER2- breast cancer; there exists clinical equipoise between the optimal strategy. The insights gleaned above prompt a re-evaluation of the conventional clinical practice to deploy CDK4/6i as front-line therapy in this setting. Instead, we raise the provocative question whether commencing treatment with PARPi instead would lead to overall better outcomes not only in the first line setting, but also establish the genomic prerequisites for more successful subsequent CDK4/6i blockade. Based on these results, the significance of this data has been recognized and serves as the impetus for EvoPAR Breast01 study (NCT assignment pending), a randomized international phase 3 clinical trial aiming to compare frontline Saruparib (a PARP1 selective inhibitor) vs standard-of-care CDK4/6i among the patients with tumors harboring HRD.

More generally, we demonstrate that pre-treatment heterozygous loss of *RB1* predicts for development of a somatic variant of the remaining allele under the selective pressure of CDK4/6i (**Fig. 5a**). This proposed mechanism mirrors Knudson's two-hit model, which seminally demonstrated that copy number loss occurs as a necessary "second hit" for oncogenesis in hereditary retinoblastoma. Conversely, haploinsufficiency of certain tumor suppressors has been postulated; particularly, preclinical models suggest that monoallelic *RB1* loss states may be sufficient for telomere instability and epithelial to mesenchymal transition signature[53,54]. Multiple studies demonstrate that *RB1* LOH does not necessarily correlate with reduced RB1 protein expression[55–57], but may be correlated with downstream E2F related gene expression changes[55,58,59].

However, if *RB1* het loss was universally sufficient for intrinsic CDK4/6i resistance, acquisition of post-treatment *RB1* variants would be evenly distributed amongst all queried pre-treatment allelic states. The enrichment of acquired *RB1* loss variants in cases where pre-treatment *RB1* het loss was evident suggests that, in at least a subset of cases, a "second hit" variant is truly necessary for the development of treatment resistance. Further efforts are needed to discern the genomic and transcriptomic context that can further refine prediction of acquired resistance.

Our study has several potential limitations. First, we focused our analysis specifically on exonic somatic variants that have previously demonstrated functional significance. This approach may fail to capture potentially consequential interactions. For instance, the functional consequences of intronic variants of *RB1* have recently been elucidated in a cohort of small cell lung cancer patients[60]. Second, given the real-world nature of this retrospective analysis, time between a particular event (i.e. start of treatment or disease progression) and a particular biopsy may vary. Our paired pre-post analysis may have failed to capture clonal expansion events which were extinguished by further therapy. Despite these caveats, we were able to conclusively demonstrate that pre-treatment *RB1* allelic configuration predicts for the development of a "second hit".

From a translational perspective, this work contributes to ongoing efforts to hasten the identification and interception of such acquired resistance mechanisms. The ability to predict the precise mechanism of acquired resistance from genomic characteristics of the pre-treatment sample is a valuable tool in the precision oncology arsenal. Currently defined "targetable" genomic lesions encompass mutations, copy number alterations, fusions which have already disrupted a specific oncogenic pathway. With this work, we propose to expand the paradigm of

the “actionable genome” to allele specific copy number alterations, allowing for earlier forecasting and intervention on fated therapeutic failure.

FIGURES

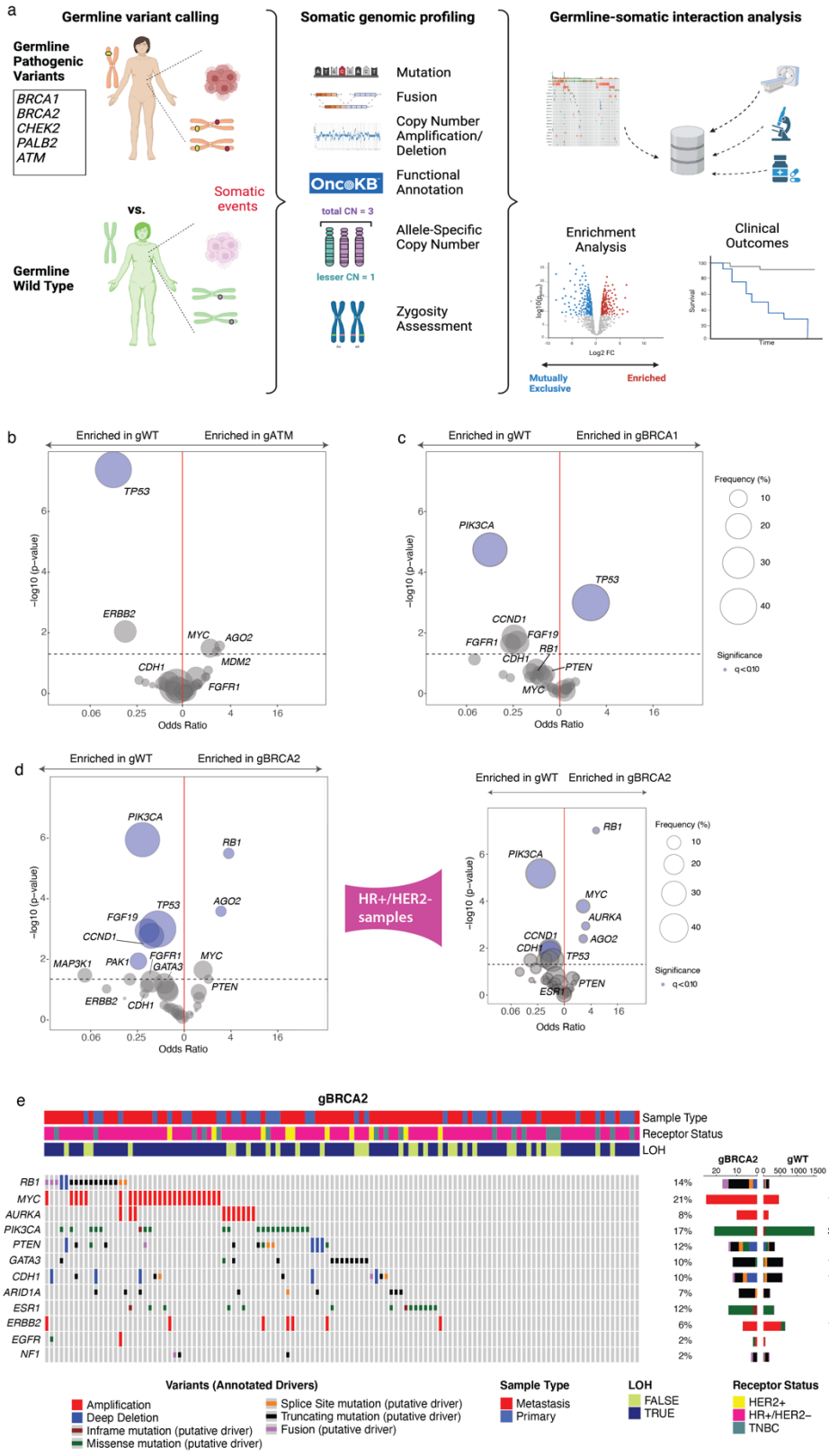
a
Germline variant calling
Germline Pathogenic Variants
BRCA1
BRCA2
CHEK2
PALB2
ATM
Somatic events
vs.
Germline Wild Type
Somatic genomic profiling
Mutation
Fusion
Copy Number Amplification/ Deletion
OncoKB
Functional Annotation
total CN = 3
lesser CN = 1
Allele-Specific Copy Number
Zygosity Assessment
Germline-somatic interaction analysis
Enrichment Analysis
Clinical Outcomes
Mutually Exclusive
Enriched
b
Enriched in gWT
Enriched in gATM
TP53
ERBB2
MYC
AGO2
MDM2
CDH1
FGFR1
−log10 (p-value)
Odds Ratio
c
Enriched in gWT
Enriched in gBRCA1
PIK3CA
TP53
CCND1
FGF19
FGFR1
RB1
CDH1
PTEN
MYC
Frequency (%)
Significance
q<0.10
d
Enriched in gWT
Enriched in gBRCA2
PIK3CA
RB1
TP53
AGO2
FGF19
CCND1
FGFR1
GATA3
MYC
MAP3K1
PAK1
PTEN
ERBB2
CDH1
HR+/HER2- samples
AURKA
ESR1
e
gBRCA2
Sample Type
Receptor Status
LOH
gWT
RB1
MYC
AURKA
PIK3CA
PTEN
GATA3
CDH1
ARID1A
ESR1
ERBB2
EGFR
NF1
Variants (Annotated Drivers)
Amplification
Deep Deletion
Inframe mutation (putative driver)
Missense mutation (putative driver)
Splice Site mutation (putative driver)
Truncating mutation (putative driver)
Fusion (putative driver)
Sample Type
Metastasis
Primary
LOH
FALSE
TRUE
Receptor Status
HER2+
HR+/HER2−
TNBC

Fig. 1: a) Study schema: we perform enrichment analysis of somatic alterations in the context of germline pathogenic variants of homologous recombination pathway (HRD) genes (compared to "sporadic" or germline wild-type cases). **b)** Results of enrichment analysis of g*BRCA1;* n = 101 compared to g*WT*; n = 4115), as determined by Firth penalized logistic regression with sample type and receptor status as covariates. Significant genes (blue) defined as q-value < 0.10. In particular, *gBRCA1* tumors were enriched for somatic *TP53* variants (2.79, (95% CI 1.59 – 4.91), q= 0.006) and mutually exclusive for *PIK3CA* variants. **c)** As in b, but depicting comparison of g*ATM,* n = 43; compared to g*WT*). **d)** As in b and c, but depicting comparison of g*BRCA2*, n = 122; compared to g*WT*, n = 4115). This is subsequently subset by HR+/HER2- cases (total n = 2910, n*BRCA2* = 93, n*WT* = 2817). Somatic *RB1* variant represent the most significant enrichment in germline *BRCA2* PVs (OR 3.31 (1.91 – 5.76, q = 0.00040) **e)** Oncoprint detailing mutation, copy number deletions, fusions in g*BRCA2* vs. g*WT*. Receptor status, sample type, and zygosity are annotated above.

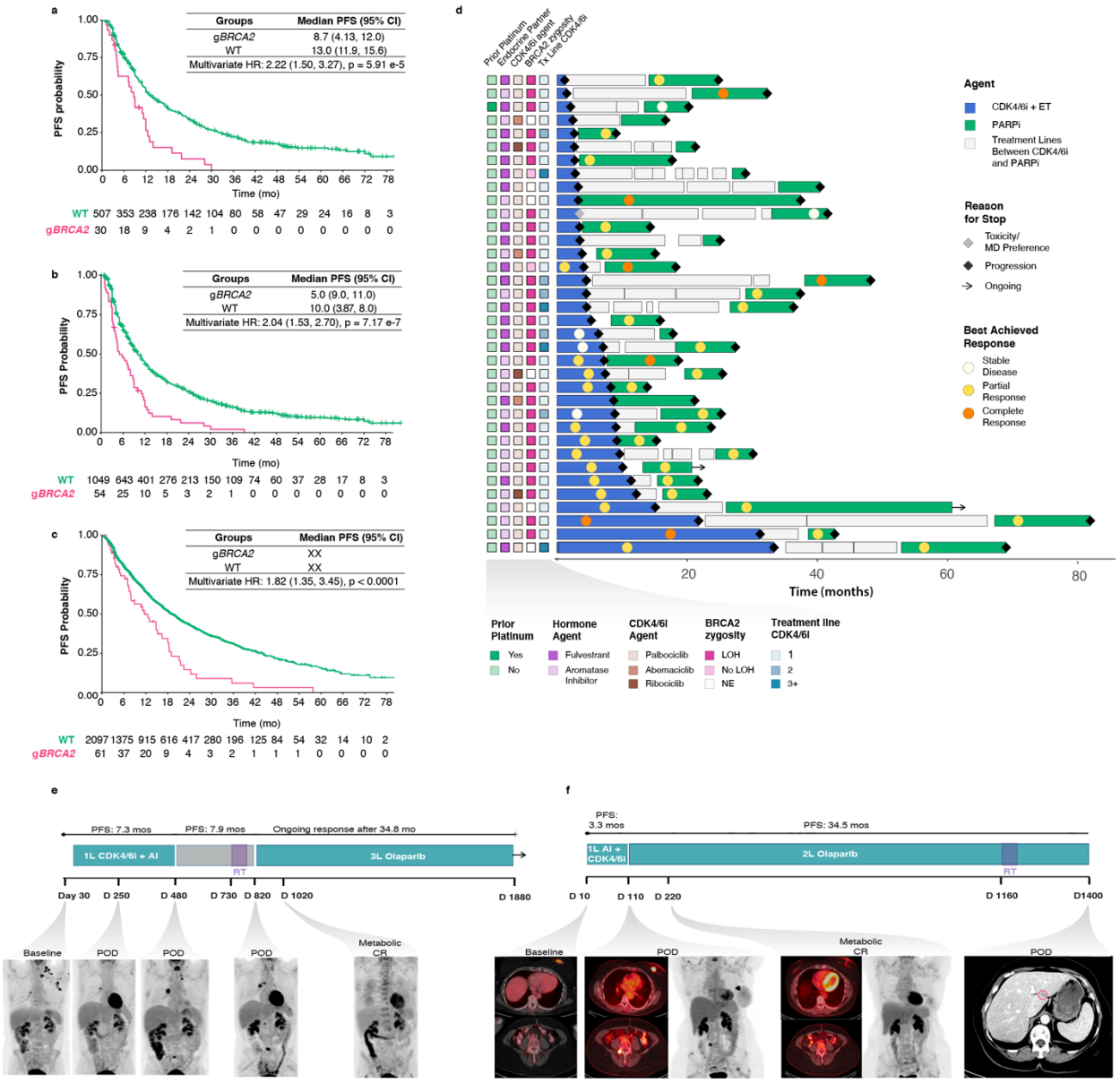

Fig. 2: a) Progression free survival to first-line CDK4/6i and endocrine therapy by g*BRCA2* status. Multivariate Cox-proportional hazard ratio, including endocrine therapy partner as covariate (hazard ratio 2.22, 95% confidence interval 1.50 – 3.27, p = 5.91 e -5) from single institution retrospective cohort. **b)** as in b, but depicting all lines of treatment; treatment line is therefore included as covariate in multivariate model (hazard ratio 2.04 (1.53 – 2.70), 8.95 e -7). **c)** Progression free survival to first-line CDK4/6i and endocrine therapy by g*BRCA2* status from multi-institutional external validation cohort (hazard ratio 1.6 (1.3 – 2.0), p < 0.01). **d)** Swimmer's plot depicting outcomes of patients receiving PARP inhibitors (green bar) after CDK4/6i and endocrine therapy (blue bar). Median PARPi/ CDK4/6i treatment duration was 1.43 (IQR 0.70 – 2.32), with paired Wilcoxon signed-rank test p = 0.091. Measured interim

response (defined as either CR; complete response or PR; partial response) on CDK4/6i vs. PARPi was assessed with Fisher's exact test; $p = 0.026$). **e,f)** Two representative cases from the above plot are highlighted, denoting short progression free interval (7.3 mos and 3.3 mos, respectively) on first-line CDK4/6i and hormonal blockade. Both patients experienced a complete metabolic response on subsequent line PARP inhibitors and have either remained on this after 34.8 mos or progressed after 34.5 mos, respectively.

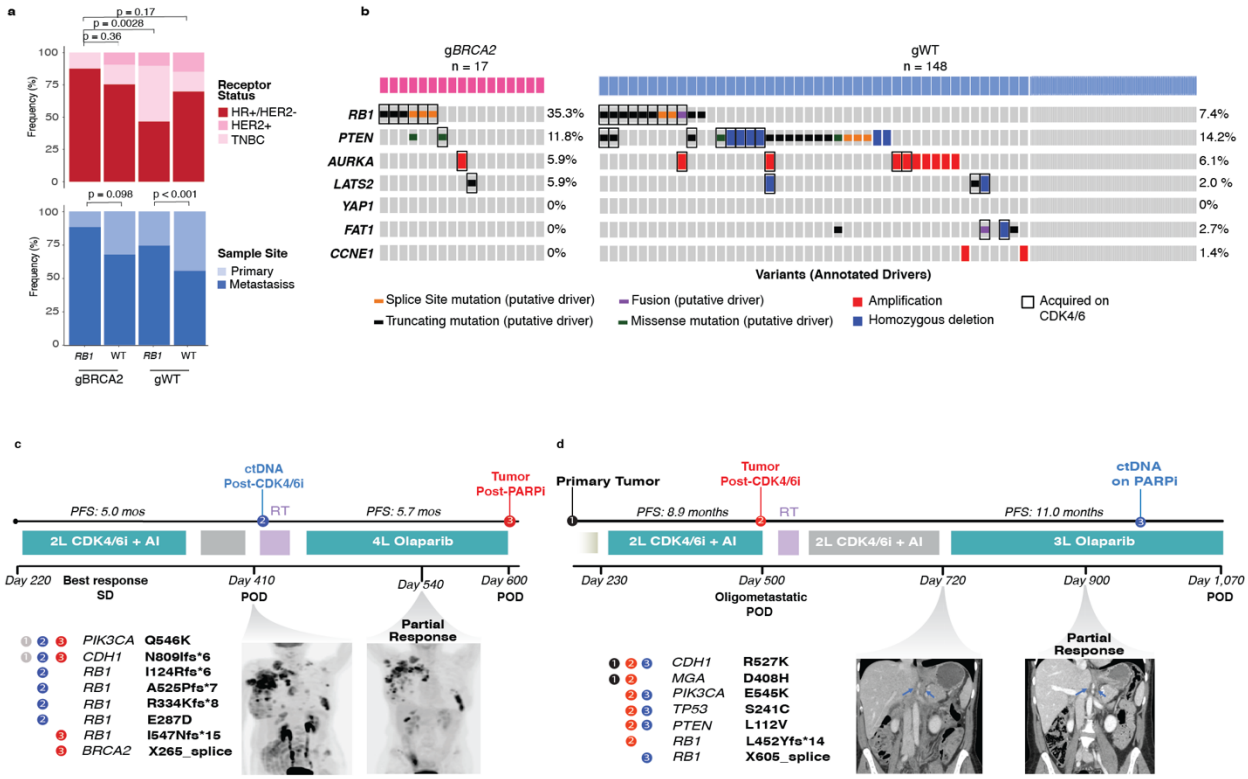

Fig. 3: a) Clinicopathological characteristics of tumors with *RB1* somatic variant vs. *RB1* wild-type, by germline *BRCA2* status. Significance bars represent results of fisher exact test to assess enrichment of i)HR+/HER2- status between the selected groups (top) and ii) metastasis and post-treatment primary vs. treatment naïve primary between selected groups. **b)** Results of paired pre and post sample analysis by germline and somatic *BRCA2* status, as well as germline *HRD*-related gene status. Oncoprint of post-CDK4/6 samples are depicted; cases where variant is not present in the pre-treatment sample outlined with black rectangle. Fisher exact test of RB1 acquisition by g*BRCA2* status: (OR 7.79, 95% CI 2.23 – 28.3, p = 0.0016. **c, d**) Two representative cases of g*BRCA2* patients with rapid progression on g*BRCA2* and prolonged responses on PARP inhibitors.

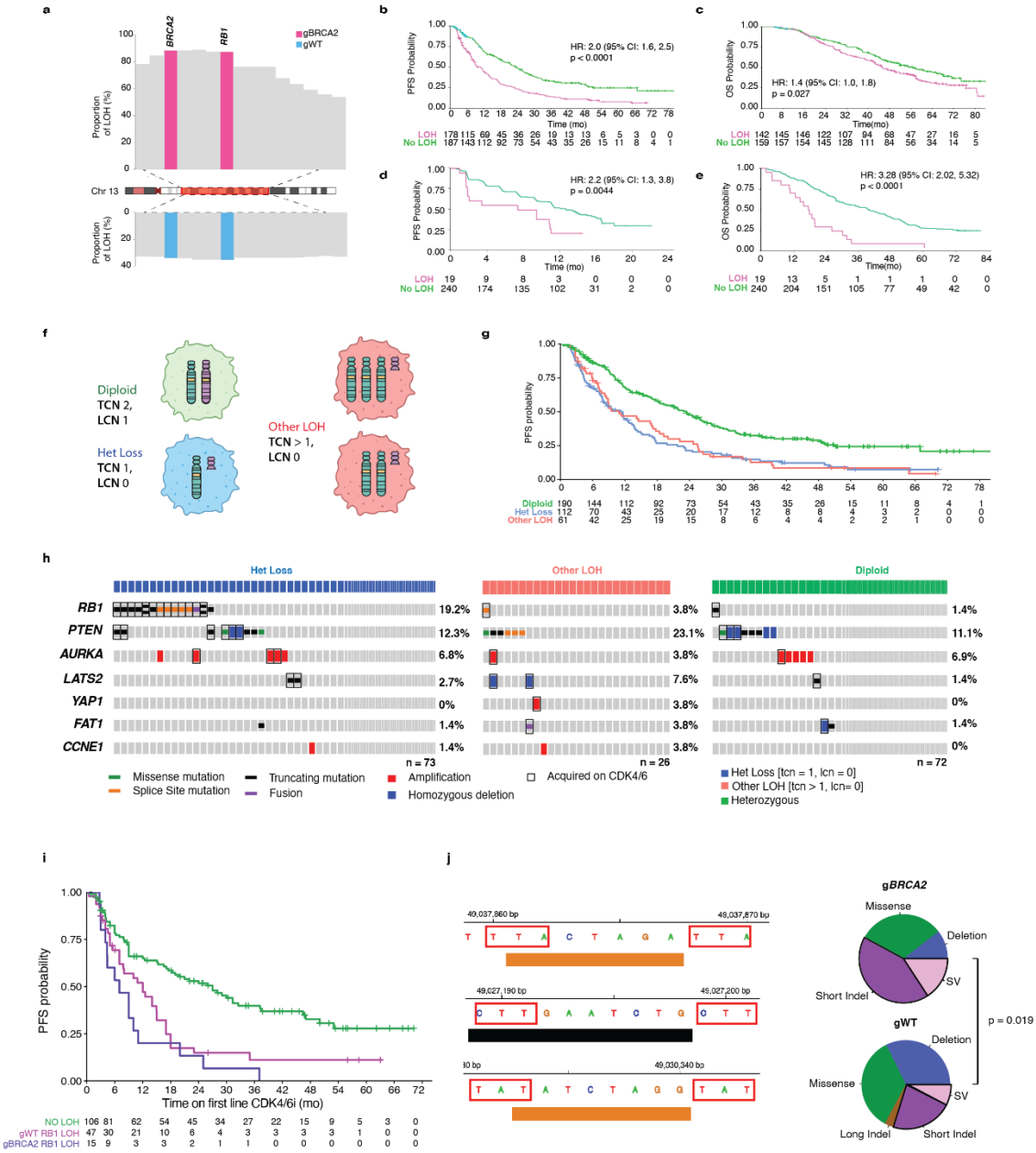

Fig. 4: Comparison of LOH frequency of chromosome 13q in g*BRCA2* pathogenic variants (top), compared to g*WT* (bottom). The same segment spans RB1 and BRCA2 in 77.2% (n = 61) of g*BRCA2* cases, while a similar phenomenon is seen in wild-type cases 28.0% (n = 495). All tumors included here are from patients classified as HR+/HER2-. b) Progression free survival to first-line CDK4/6i and endocrine therapy by pre-treatment RB1 LOH status, from MSK cohort. Multivariate Cox-proportional hazard ratio, including endocrine therapy partner as covariate (hazard ratio 1.94, 95% confidence interval 1.52 – 2.48, p = 1.21 e -7). c) as in e, but reporting overall survival. The survival time is left -truncated to prevent immortality bias from the time of metastatic recurrence to the time of inclusion on the prospective sequencing protocol. Hazard ratio for overall survival 1.34 (1.01 – 1.78), p =0.04. d) as in e, but reporting progression free

survival results from sequencing of baseline circulating tumor DNA from PALOMA-3. Hazard ratio 2.20 (1.26 – 3.82), p = 0.0055. e) as in g, but depicting overall survival. Hazard ratio 3.28 (2.02 – 5.32), p < 0.001. f) Schematic representation of various copy number states that are included in the traditional definition of "*RB1* LOH*"*. This includes tumors not only with one total remaining allele (het loss, blue), but also cases with two or greater uniparental copies of the maternal or paternal allele (red). g) Progression free survival to first-line CDK4/6i and endocrine therapy by refined allele-specific RB1 copy number status, from MSK cohort. Multivariate Cox-proportional hazard ratio, including endocrine therapy partner as covariate. (hazard ratio of RB1 het loss group: 1.98 (1.51 – 2.61), p = 1.08 e -6; hazard ratio of RB1 other LOH = 1.89 (1.35 – 2.61), p = 0.00018). h) Results of paired pre and post sample analysis by pre-allelic status. Oncoprint of post-CDK4/6 samples are depicted; cases where variant is not present in the pre-treatment sample outlined with black rectangle. Cases with more than one post-CDK4/6i variant in the same gene are indicated with two vertical variants. Fisher exact test of RB1 acquisition by g*BRCA2* status:(OR 10,3, 95% CI 2.30 – 65.7, p = 0.00050). i) Progression free survival to first-line CDK4/6i and endocrine therapy by RB1 LOH status and gBRCA2 status. j) Left: Nucleotide context of select RB1 variants in g*BRCA2*-associated tumors, depicting short indel flanked by regions of microhomology. Right: Comparison of putative HRD-associated somatic variants of *RB1* (short indels, defined as < 25 bp, and structural variants) by g*BRCA2* status. Fisher exact test : P = 0.019.

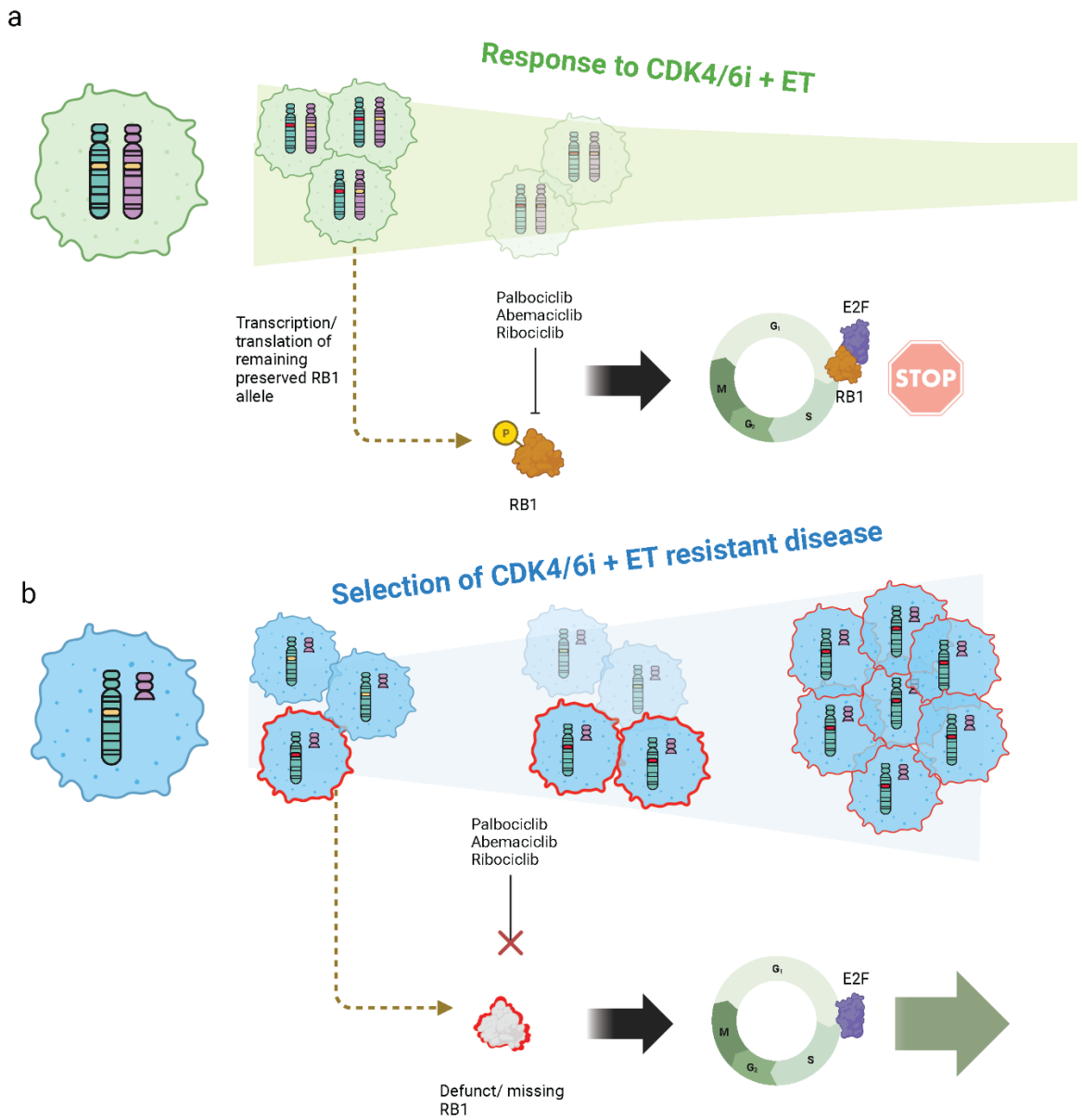

Fig. 5) Our data demonstrates that pre-treatment allelic configuration of *RB1* influences treatment duration on CDK4/6i and endocrine therapy while also predicting for the precise mechanism of resistance. To explain this, we posit that a single copy loss of *RB1* which may occur through single allelic loss-of-function mutation in an otherwise diploid setting (*RB1*-mu*t*/*RB1*-WT) is not sufficient to confer resistance to CDK4/6i. Therefore, tumors with two or more copies of *RB1* (e.g. diploid state, represented in *green*: *RB1*-WT/*RB1*-WT, top) are relatively less likely to develop complete loss of *RB1*.

Conversely, breast cancers with only one allele present pre-treatment (*RB1* het loss or *RB1*-WT/*RB1*-loss, depicted in *blue)* experience complete *RB1* loss upon loss of function variant affecting the remaining allele. Therefore, this *RB1*-mut/*RB1*-loss clone may expand under the selective pressure of CDK4/6i and endocrine therapy, resulting in disease progression.

Table 1

	ATM (N=45)	BRCA1 (N=105)	BRCA2 (N=127)	CHEK2 (N=63)	PALB2 (N=25)	WT (N=4285)	P-value
Age at Diagnosis							<0.001
<= 35	6 (13.3%)	37 (35.2%)	27 (21.3%)	8 (12.9%)	2 (8.0%)	375 (9.2%)	
36-50	22 (48.9.2%)	33 (31.4%)	50 (39.4%)	27 (43.5%)	13 (52.0%)	1543 (37.7%)	
51-60	4 (8.9%)	13 (12.4%)	28 (22.4%)	15 (24.2%)	5 (20.0%)	1127 (27.5%)	
61-70	8 (17.8%)	9 (8.6%)	11 (8.7%)	8 (12.9%)	2 (8.0%)	769 (18.8%)	
> 70	3 (6.7%)	5 (4.8%)	2 (1.6%)	4 (6.5%)	1 (4.0%)	281 (6.9%)	
Unknown	2 (4.4%)	8 (7.6%)	9 (7.1%)	1 (1.6%)	2 (8.0%)	190 (4.4%)	
Menopausal Status At Diagnosis							<0.001
Post	15 (33.3%)	28 (26.6%)	37 (29.1%)	19 (30.2%)	6 (24.0%)	2010 (46.9%)	
Pre/ Peri	28 (62.2%)	68 (64.8%)	71 (55.9%)	40 (63.5%)	16 (64.0%)	1982 (46.3%)	
Not Applicable (Male)	0 (0%)	1 (0.9%)	5 (3.9%)	1 (1.6%)	0 (0%)	34 (0.8%)	
Unknown	2 (4.4%)	8 (7.6%)	14 (11.8%)	3 (4.8%)	3 (12.0%)	259 (6.3%)	
Receptor Status							<0.001
HER2+	8 (17.8%)	4 (3.8%)	10 (7.9%)	9 (14.3%)	1 (4.0%)	589 (13.7%)	
HR+/HER2-	34 (75.6%)	29 (27.6%)	90 (71.0%)	47 (74.6%)	15 (60.0%)	2814 (65.7%)	
TNBC	1 (2.2%)	64 (61.0%)	18 (14.2%)	6 (9.5%)	7 (28.0%)	678 (15.8%)	
Unknown	2 (4.4%)	8 (7.6%)	9 (7.1%)	1 (1.6%)	2 (8.0%)	190 (4.4%)	
Overall Histologic Grade							<0.001
I Low Grade (Well Differentiated)	0 (0%)	0 (0%)	0 (0%)	3 (4.8%)	2 (8.0%)	163 (3.8%)	
II Intermediate Grade (Moderately Differentiated)	10 (22.2%)	7 (6.7%)	28 (22.0%)	18 (28.6%)	8 (32.0%)	911 (21.2%)	
III High Grade (Poorly Differentiated)	25 (55.6%)	84 (80.0%)	74 (58.3%)	32 (50.8%)	10 (40.0%)	2571 (60.0%)	
Missing	10 (22.2%)	14 (13.3%)	25 (19.7%)	10 (15.9%)	5 (25.0%)	450 (11.0%)	

	ATM (N=45)	BRCA1 (N=105)	BRCA2 (N=127)	CHEK2 (N=63)	PALB2 (N=25)	WT (N=4285)	P-value
Histology							0.0139
Invasive Ductal Carcinoma	34 (75.6%)	89 (84.8%)	93 (73.2%)	49 (77.8%)	19 (76%)	3232 (75.4%)	
Invasive Lobular Carcinoma	4 (8.9%)	3 (2.9%)	10 (7.8%)	6 (9.5%)	2 (8.0%)	511 (11.9%)	
Mixed/ Other	5 (11.1%)	5 (4.8%)	15 (11.8%)	7 (11.1%)	2 (8.0%)	352 (8.21%)	
Unknown	2 (4.4%)	8 (7.6%)	9 (7.1%)	1 (1.6%)	2 (8.0%)	190 (4.4%)	
Stage at Diagnosis							0.0103
I	11 (24.4%)	34 (32.4%)	25 (19.7%)	16 (25.4%)	11 (44.0%)	1103 (25.7%)	
II	7 (15.6%)	39 (37.1%)	37 (29.1%)	21 (33.3%)	5 (20.0%)	1370 (32.0%)	
III	6 (13.3%)	9 (8.6%)	22 (17.3%)	7 (11.1%)	2 (8.0%)	692 (16.1%)	
IV	13 (28.9%)	10 (9.5%)	29 (22.8%)	16 (25.4%)	3 (12.0%)	733 (17.1%)	
Unknown	8 (17.8%)	13 (12.4%)	14 (11.0%)	3 (4.8%)	4 (16.0%)	387 (90%)	

METHODS:

Study cohort and prospective sequencing

The study cohort comprised 5,601 samples from 4,640 patients. All patients underwent prospective clinical sequencing as part of their clinical care (February 2014 to July 2017). The present study was approved by the MSK Cancer Center's Institutional Review Board (IRB) and all patients provided written informed consent for tumor sequencing and review of medical records for demographic, clinical and pathology information. Genomic sequencing was performed on tumor DNA extracted from formalin-fixed, paraffin-embedded tissue and normal DNA extracted from mononuclear cells from peripheral blood in all patients. Patient samples were sequenced in a CLIA-compliant laboratory during routine clinical testing, using one of three versions of the MSK-IMPACT-targeted sequencing panel, which included 341- and 410-gene versions and the current 468-gene FDA-authorized panel using methods and somatic analysis described previously. Tumors were obtained from the primary site in 50.8% of cases and from a metastatic site in 49.2% of cases.

Germline variant calling was performed using a sequence analysis pipeline validated for clinical use in a CLIA-compliant laboratory performing clinical sequencing of patient tumors and matched normal blood specimens as a part of routine clinical care. To identify pathogenic germline variants related to cancer, we employed a machine learning-based methodology previously described in Srinivasan et al. Briefly, this framework incorporated mutation type, functional gene class, population allele frequencies, and orthogonal in silico tools to predict functional impact, and was trained on a cohort of 6,009 patients with cancer whose germline data were prospectively curated by expert clinical molecular geneticists using American College of

Medical Genetics guidelines for clinical interpretation. This framework was applied to a cohort of breast cancer patients at our institution who underwent prospective clinical genomic profiling under our sequencing protocol from April 2015 to August 2019 (n = 4640). Demographics, pathologic (including subsequent tumor sequencing data) and detailed clinical information was collected until date of data freeze (September 2021). Low-risk variants in CHEK2 such as p.Ile157Thr were excluded from the analysis.

A total of 1927 patients had consented for identified analysis of germline variants via an IRB protocol (NT01775072). Genomic and limited clinical data for all other patients analyzed in the present study (n = 2695) were anonymized before germline variant discovery and subsequent analyses. For numerical variables (such as time on treatment), this entailed rounding to the nearest digit; treatment times were therefore rounded to the nearest month. All single-nucleotide variants and small insertions and deletions (indels) identified in any blood normal sample were annotated with myvariant.info (as of August 2017)43. Population frequencies were obtained from gnomAD (r2.0.2)44. Curated assessments for pathogenicity were obtained from ClinVar (as of September 2017)45.

Zygosity inference

We inferred somatic zygosity for all germline pathogenic variants using locus- and allele-specific DNA copy number inference (cite FACETS). All allele specific copy number (ASCN) solutions (FACETS outputs) from tumors with germline pathogenic variants were manually reviewed to ensure appropriate solutions. Purity estimates were similarly inferred from the FACETS solution. We incorporated ASCN, purity and variant allele frequency into a previously described (Jonsson

et al) framework, allowing statistical inference of heterozygous, biallelic (loss of wild type allele), or loss of mutant allele. The zygosity of the germline variant was considered indeterminate and excluded from zygosity analyses if the: (1) variant was homozygous in the germline; (2) read depth of coverage in the normal blood specimen was <50; (3) FACETS-derived total and minor copy number were not evaluable at the corresponding locus, or (4) Optimal FACETS solution was not able to be identified, most commonly from due to tumor purity issues. Using this criteria, out of the 386 total cases with germline PV in the genes of interest, somatic zygosity status was evaluable for 312 (80.8%) of tumors. Additionally, we excluded cases where copy number analysis and variant allele frequency was suggestive of loss of mutant allele, rather than wild type (n = 27, 7.90%) from further analyses.

To initially determine whether a given germline variant is in allelic imbalance in the corresponding tumor specimen, we evaluated consistency between observed somatic VAF and expected VAF. The latter value is calculated as a function of allele-specific DNA copy number and purity as follows:

$$\Phi\times mcn+(1-\Phi)\Phi\times tcn+2\times(1-\Phi)\Phi\times mcn+(1-\Phi)\Phi\times tcn+2\times(1-\Phi)$$

where ϕ is the tumor purity and tcn and lcn are the total and lesser copy number at the locus spanning the variant. Germline variants were considered heterozygous if their observed VAF was either (1) consistent with the expected VAF (within its 95% binomial CI) given balanced heterozygosity (tcn and mcn of either 2 and 1 or 4 and 2 in diploid and genome doubled tumors, respectively), or (2) less than the lower bound of the 95% CI of the expected VAF corresponding to a tcn and mcn of 3 and 1, respectively, which was either single copy gain of the mutant or WT allele. Germline variants in allelic imbalance of any kind were those with an observed VAF that

was either within or greater than the 95% CI of the expected VAF corresponding to a copy-number state other than balanced heterozygosity[56]. For allelically imbalanced germline variants, loss of the WT was determined as those with an observed VAF within the 95% CI (or greater than the lower bound of the 95% CI) of the expected VAF corresponding to an lcn equal to 0 (observed VAF is concordant with the expected VAF when the lesser allele has a copy number of 0).

Clinical data annotation

Detailed treatment history data were obtained for each of patients and included all lines of systemic therapy from the time of diagnosis to the study data lock (June 2022). The exact regimen, dates of start and stop therapy, as well as date of progression was annotated via expert review.

Each patient in our cohort was assigned a singular receptor status. Recognizing potential intertumoral heterogeneity, we sought a unified definition as follows: i) in cases where any metastatic biopsy was sequenced, receptor status was defined by treating clinician interpretation and assigned first-line treatment; ii) in cases where only a primary tumor is sequenced, receptor status was defined by receptor status of the sequenced primary. We excluded cases where sequencing was obtained for external consultation (and therefore, lacked clinical or pathological data, n = 176), DCIS (n = 1), or cases where multi-site sequencing demonstrated no intra-patient genomic overlap and multiple distinct receptor statuses (n = 4) (**Fig. S1A)**. Employing these definitions, our cohort consisted of 3046 patients (68.3%) with hormone receptor positive, HER2-neu non-overexpressed (HR+/HER2-) receptor status, 781 patients (17.5%) with triple

negative breast cancer (TNBC), while the remainder (638, 14.2%) were HER2 amplified (HER2+).

Progression events were defined as i) radiographic or clinical event prompting change in systemic therapy or recommendation for locally targeted radiation therapy, ii) documented clinician impression detailing progression, after which there was documented patient or MD preference to continue same therapy. For samples who were not consented to our germline sequencing protocol (IMPACT part C), clinical outcomes were anonymized to avoid identification per institutional protocol. Outcome data (progression free survival, overall survival) was rounded to the nearest month. For samples who were consented to our institutional protocol, outcomes were not rounded.

Enrichment Analysis:

We compiled mutations, fusions, copy number alterations predicted to be functionally significant by a manually curated precision oncology variant database (Chakravarty et al). All putative *RB1* homozygous deletions were manually re-reviewed prior to anonymization. Cases where the putative homozygous deletion spanned beyond the size of an amplicon (i.e. an event which would be interpreted as incompatible with tumor survival) were flagged.

In cases where a patient had multiple samples sequenced, we compiled the total somatic variants called from either the sequenced primary sample or all sequenced metastatic samples (omitting the primary), in order to avoid duplicate samples and to ensure that each set of variants was assigned either “primary” or “metastasis” as a covariate. Upon excluding samples with

indeterminable receptor status (as described in “clinical data annotation” section), 4459 patients were eligible for Firth-penalized logistic regression.

Receptor status was also defined on a “per-patient” as described above. Genes with alterations in less than 2% of patients were omitted from the analysis. For each remaining combination of germline gene X and somatic gene Y, we performed a Firth penalized logistic regression to account for the sparsity of the dataset. Receptor status and sample type (metastatic vs. primary) were included as covariates. The analysis was also repeated for each receptor status subtype, as well as repeated for biallelic vs mono-allelic germline variants. The latter step was only performed for samples where zygosity was evaluable (n = 4398). Putative p-values were adjusted for multiple hypothesis testing using the Benjamini-Hochberg method.

Allele-Specific Copy Number Definitions

In the MSK cohort, somatic loss of heterozygosity events of *RB1* were defined based on manual FACETS review of pre-CDK4/6i treatment samples. Of 470 patients with pre first line CDK4/6i biopsies, 104 were removed due to: low purity or other technical limitations (such as “waterfalling” artifact), or paucity of heterozygous SNPs allowing for confident lesser copy number inference. RB1 loss of heterozygosity was coarsely defined as lesser copy number of zero, irrespective of total copy number, while heterozygous state was any lesser copy number greater than or equal to one. In the PALOMA-3 cohort, RB1 LOH was defined as previously described in O’Leary et al Cancer Discovery.

In the MSK cohort, we further separated the *RB1* LOH group into i) heterozygous loss ("Het Loss", defined as a state with total copy number of one and lesser copy number of zero) and ii) other LOH (defined as LOH, but with total copy number greater than one). Fraction genome altered (FGA) was also calculated for each pre-treatment sample, and defined as the fraction of log2 copy number variation (gain or loss) > 0.2 divided by the total size of the copy number profiled region (Zhou CCR, Jones last author).

Clinical Outcome Analysis:

We determined the association between genomic alterations and PFS with disease progression on therapy with CDK4/6 inhibitors or patient death. We categorized CDK4/6 inhibitor regimens based on their endocrine therapy partner (aromatase inhibitor vs selective estrogen receptor degrader/ SERD). Patients with ablation of known sites of disease with radiotherapy or surgical resection prior to initiation of CDK4/6i therapy were excluded, as were patients who discontinued therapy due to toxicity after two weeks (n = 124). To maximize statistical power for downstream clinicogenomic analyses, we expanded the cohort to include CDK4/6i outcomes on all additional germline *BRCA2* pathogenic variants identified through our institutional germline pathogenic variant database (end date: 8/2022, resulting in 23 additional samples).

We employed both univariate and multivariate Cox proportional hazard models (stratified by endocrine therapy partner, and treatment line, where available). For patients with multiple lines of therapy from the same class of treatment, only the first treatment line from that class that was started after the MSK-IMPACT biopsy was included in the analysis.

For overall survival analysis, we implemented a left-truncated model to account of time from diagnosis of metastatic disease to enrollment on sequencing protocol. Similarly to the univariate analyses, we employed univariate and multivariate Cox proportional hazard models. In addition to endocrine therapy partner, age at metastatic diagnosis was also included as a covariate. We rejected the null hypotheses with a two-sided $\alpha = 0.05$.

To accomplish the matched pairs analysis, we considered any paired pre-CDK4/6i and post-CDK4/6i treatment solid tumor samples sequenced on MSK-IMPACT. Allele-specific copy number analysis was performed for the pre-treatment cases; cases where low purity precluded confident allele specific copy number ascertainment were excluded. The exclusion of such low purity samples assures acquisition of post-treatment variants is due to tumor evolution rather than technical inability to capture the preceding variant. If multiple adequate pre-treatment samples were included, each allele-specific copy number analysis

For other exploratory analyses (comparison of sample type and receptor status by RB1:BRCA2 co-mutation status, comparison of rates of RB1 loss-of-function sample acquisition by group, comparison of RB1 short indels and SVs by BRCA2 status, etc), details of statistical analysis can be found in the respective Fig. legend. Unless stated otherwise, statistical analysis of differences between samples was performed using two-tailed Fisher exact tests; $p < 0.05$ was defined as significant.

To estimate cancer cell fraction (CCF), the FACETS output of focal-copy number changes, purity and ploidy was employed, along with methods established previously[46,47]. For estimation

of CCF from ctDNA samples (MSK-ACCESS), allele-specific copy number was incorporated in this estimation from a corresponding matched tumor biopsy. The biopsy-matched clonal mutations were used to estimate the plasma sample ctDNA fraction based on the plasma variant allele frequency.

References

1. Garber, J. E. & Offit, K. Hereditary cancer predisposition syndromes. *Journal of Clinical Oncology* **23**, (2005).
2. Rahman, N. Realizing the promise of cancer predisposition genes. *Nature* **505**, (2014).
3. Antoniou, A. *et al.* Average risks of breast and ovarian cancer associated with BRCA1 or BRCA2 mutations detected in case series unselected for family history: A combined analysis of 22 studies. *Am. J. Hum. Genet.* **72**, (2003).

4. Kamieniak, M. M. *et al.* DNA copy number profiling reveals extensive genomic loss in hereditary BRCA1 and BRCA2 ovarian carcinomas. *Br. J. Cancer* **108**, (2013).

5. Stefansson, O. A. *et al.* Genomic profiling of breast tumours in relation to BRCA abnormalities and phenotypes. *Breast Cancer Res.* **11**, (2009).

6. Lynch, C. J. & Milner, J. Loss of one p53 allele results in four-fold reduction of p53 mRNA and protein: A basis for p53 haplo-insufficiency. *Oncogene* **25**, (2006).

7. Knudson, A. G. Hereditary cancer: Two hits revisited. *Journal of Cancer Research and Clinical Oncology* (1996). doi:10.1007/BF01366952

8. Nichols, K. E., Malkin, D., Garber, J. E., Fraumeni, J. & Li, F. P. Germ-line p53 mutations predispose to a wide spectrum of early-onset cancers. *Cancer Epidemiol. Biomarkers Prev.* **10**, (2001).

9. Knudson, A. G., Meadows, A. T., Nichols, W. W. & Hill, R. Chromosomal Deletion and Retinoblastoma. *N. Engl. J. Med.* **295**, (1976).

10. Hyman, D. M., Taylor, B. S. & Baselga, J. Implementing Genome-Driven Oncology. *Cell* **168**, (2017).

11. Qing, T. *et al.* Germline variant burden in cancer genes correlates with age at diagnosis and somatic mutation burden. *Nat. Commun.* (2020). doi:10.1038/s41467-020-16293-7

12. Srinivasan, P. *et al.* The context-specific role of germline pathogenicity in tumorigenesis. *Nat. Genet.* **53**, (2021).

13. Holstege, H. *et al.* High Incidence of Protein-Truncating TP53 Mutations in BRCA1-Related Breast Cancer. *Cancer Res* **69**, 3625–3658 (2009).

14. Greenblatt, M. S., Chappuis, P. O., Bond, J. P., Hamel, N. & Foulkes, W. D. TP53 mutations in breast cancer associated with BRCA1 or BRCA2 germ-line mutations: Distinctive spectrum and structural distribution. *Cancer Res.* **61**, (2001).

15. Weigelt, B. *et al.* Diverse BRCA1 and BRCA2 reversion mutations in circulating cell-free DNA of therapy-resistant breast or ovarian cancer. *Clin. Cancer Res.* (2017). doi:10.1158/1078-0432.CCR-17-0544

16. Mareckova, A. *et al.* ATM and TP53 mutations show mutual exclusivity but distinct clinical impact in mantle cell lymphoma patients. *Leuk. Lymphoma* **60**, (2019).

17. Robson, M. *et al.* Olaparib for metastatic breast cancer in patients with a germline BRCA mutation. *N. Engl. J. Med.* (2017). doi:10.1056/NEJMoa1706450

18. Litton, J. K. *et al.* Talazoparib in Patients with Advanced Breast Cancer and a Germline *BRCA* Mutation. *N. Engl. J. Med.* **379**, 753–763 (2018).

19. Vasan, N., Baselga, J. & Hyman, D. M. A view on drug resistance in cancer. *Nature* **575**, (2019).

20. Mavaddat, N. *et al.* Pathology of breast and ovarian cancers among BRCA1 and BRCA2 mutation carriers: Results from the consortium of investigators of modifiers of BRCA1/2

(CIMBA). *Cancer Epidemiol. Biomarkers Prev.* **21**, (2012).

21. Hortobagyi, G. N. *et al.* Ribociclib as First-Line Therapy for HR-Positive, Advanced Breast Cancer. *N. Engl. J. Med.* **375**, (2016).

22. Cristofanilli, M. *et al.* Fulvestrant plus palbociclib versus fulvestrant plus placebo for treatment of hormone-receptor-positive, HER2-negative metastatic breast cancer that progressed on previous endocrine therapy (PALOMA-3): final analysis of the multicentre, double-blind, phase 3 randomised controlled trial. *Lancet Oncol.* **17**, (2016).

23. Goetz, M. P. *et al.* MONARCH 3: Abemaciclib As Initial Therapy for Advanced Breast Cancer. *J. Clin. Oncol.* **35**, 3638–3646 (2017).

24. Cheng, D. T. *et al.* Memorial Sloan Kettering-Integrated Mutation Profiling of Actionable Cancer Targets (MSK-IMPACT). *J. Mol. Diagnostics* (2015). doi:10.1016/j.jmoldx.2014.12.006

25. Zehir, A. *et al.* Mutational landscape of metastatic cancer revealed from prospective clinical sequencing of 10,000 patients. *Nat. Med.* **23**, 703–713 (2017).

26. Razavi, P. *et al.* The Genomic Landscape of Endocrine-Resistant Advanced Breast Cancers. *Cancer Cell* **34**, 427-438.e6 (2018).

27. Chen, H. *et al.* Association between BRCA status and triple-negative breast cancer: A meta-analysis. *Front. Pharmacol.* **9**, 909 (2018).

28. Krammer, J. *et al.* Breast cancer detection and tumor characteristics in BRCA1 and BRCA2 mutation carriers. *Breast Cancer Res. Treat. 2017 1633* **163**, 565–571 (2017).

29. Goodwin, P. J. *et al.* Breast cancer prognosis in BRCA1 and BRCA2 mutation carriers: An international prospective breast cancer family registry population-based cohort study. *J. Clin. Oncol.* **30**, 19–26 (2012).

30. Brekelmans, C. T. M. *et al.* Tumour characteristics, survival and prognostic factors of hereditary breast cancer from BRCA2-, BRCA1- and non-BRCA1/2 families as compared to sporadic breast cancer cases. *Eur. J. Cancer* **43**, 867–876 (2007).

31. Maxwell, K. N. *et al.* BRCA locus-specific loss of heterozygosity in germline BRCA1 and BRCA2 carriers. *Nat. Commun.* **8**, 1–11 (2017).

32. Riaz, N. *et al.* Pan-cancer analysis of bi-allelic alterations in homologous recombination DNA repair genes. *Nat. Commun.* (2017). doi:10.1038/s41467-017-00921-w

33. Li, A. *et al.* Homologous recombination DNA repair defects in PALB2-associated breast cancers. *npj Breast Cancer 2019 51* **5**, 1–14 (2019).

34. Chakravarty, D. *et al.* OncoKB: A Precision Oncology Knowledge Base. *JCO Precis. Oncol.* **1**, 1–16 (2017).

35. Maxwell, K. N. *et al.* BRCA locus-specific loss of heterozygosity in germline BRCA1 and BRCA2 carriers. *Nat. Commun. 2017 81* **8**, 1–11 (2017).

36. Na, B. *et al.* Therapeutic targeting of BRCA1 and TP53 mutant breast cancer through

mutant p53 reactivation. *npj Breast Cancer 2019 51* **5**, 1–10 (2019).

37. Brugarolas, J. & Jacks, T. Double indemnity: p53, BRCA and cancer. p53 mutation partially rescues developmental arrest in Brca1 and Brca2 null mice, suggesting a role for familial breast cancer genes in DNA damage repair. *Nat. Med.* **3**, 721–722 (1997).

38. Ghezelayagh, T. S. *et al.* Characterizing TP53 mutations in ovarian carcinomas with and without concurrent BRCA1 or BRCA2 mutations. *Gynecol. Oncol.* **160**, 786–792 (2021).

39. Wander, S. A. *et al.* The genomic landscape of intrinsic and acquired resistance to cyclin-dependent kinase 4/6 inhibitors in patients with hormone receptor–positive metastatic breast cancer. *Cancer Discov.* **10**, (2020).

40. Scheidemann, E. R. & Shajahan-Haq, A. N. Resistance to CDK4/6 inhibitors in estrogen receptor-positive breast cancer. *International Journal of Molecular Sciences* **22**, (2021).

41. Kim, S. *et al.* Sequential activation of E2F via Rb degradation and c-Myc drives resistance to CDK4/6 inhibitors in breast cancer. *Cell Rep.* **42**, (2023).

42. Li, Z. *et al.* Loss of the FAT1 Tumor Suppressor Promotes Resistance to CDK4/6 Inhibitors via the Hippo Pathway. *Cancer Cell* (2018). doi:10.1016/j.ccell.2018.11.006

43. Ma, X. *et al.* Comparison of Population Characteristics in Real-World Clinical Oncology Databases in the US: Flatiron Health, SEER, and NPCR. *medRXiv* (2023). doi:10.1101/2020.03.16.20037143

44. Kainu, T. *et al.* Somatic deletions in hereditary breast cancers implicate 13q21 as a putative novel breast cancer susceptibility locus. *Proc. Natl. Acad. Sci. U. S. A.* **97**, 9603–9608 (2000).

45. Rouault, A. *et al.* Deletion of chromosomes 13q and 14q is a common feature of tumors with BRCA2 mutations. *PLoS One* **7**, (2012).

46. O'leary, B. *et al.* Circulating Tumor DNA Markers for Early Progression on Fulvestrant With or Without Palbociclib in ER+ Advanced Breast Cancer. *JNCI J. Natl. Cancer Inst.* **113**, 309–317 (2021).

47. Turner, Nicholas C., Dennis J. Slamon, Jungsil Ro, Igor Bondarenko, Seock-Ah Im, Norikazu Masuda, M. C. Overall survival with palbociclib and fulvestrant in advanced breast cancer. *N. Engl. J. Med.* **349**, 1926–36 (2018).

48. Bielski, C. M. *et al.* Genome doubling shapes the evolution and prognosis of advanced cancers. *Nat. Genet. 2018 508* **50**, 1189–1195 (2018).

49. André, F. *et al.* Pooled ctDNA analysis of MONALEESA phase III advanced breast cancer trials. *Ann. Oncol.* (2023). doi:10.1016/j.annonc.2023.08.011

50. Soria-Bretones, I. *et al.* The spindle assembly checkpoint is a therapeutic vulnerability of CDK4/6 inhibitor–resistant ER+ breast cancer with mitotic aberrations. *Sci. Adv.* **8**, (2022).

51. Gong, X. *et al.* Aurora a kinase inhibition is synthetic lethal with loss of the RB1 tumor suppressor gene. *Cancer Discov.* **9**, (2019).

52. Gould, S. J. & Vrba, E. S. Exaptation—a Missing Term in the Science of Form. *Paleobiology* **1**, (1982).

53. Chakraborty, G. *et al.* Significance of BRCA2 and RB1 co-loss in aggressive prostate cancer progression. *Clin. Cancer Res.* (2020). doi:10.1158/1078-0432.CCR-19-1570

54. Gonzalez-Vasconcellos, I. *et al.* The Rb1 tumour suppressor gene modifies telomeric chromatin architecture by regulating TERRA expression. *Sci. Rep.* **7**, (2017).

55. Herschkowitz, J. I., He, X., Fan, C. & Perou, C. M. The functional loss of the retinoblastoma tumour suppressor is a common event in basal-like and luminal B breast carcinomas. *Breast Cancer Res.* **10**, R75 (2008).

56. Bieche, I., Champeme, M. H. & Lidereau, R. International journal of cancer. Journal international du cancer. *Int J Cancer* **82**, 908–910 (1999).

57. Borg, A., Zhang, Q. X., Alm, P., Olsson, H. & Sellberg, G. The retinoblastoma gene in breast cancer: allele loss is not correlated with loss of gene protein expression. *Cancer Res.* **52**, 2991–2994 (1992).

58. Knudsen, E. S. *et al.* Pan-cancer molecular analysis of the RB tumor suppressor pathway. *Commun. Biol. 2020 31* **3**, 1–12 (2020).

59. Xia, Y., Fan, C., Hoadley, K. A., Parker, J. S. & Perou, C. M. Genetic determinants of the molecular portraits of epithelial cancers. *Nat. Commun. 2019 101* **10**, 1–13 (2019).

60. Febres-Aldana, C. *et al.* Rb Tumor Suppressor in Small Cell Lung Cancer: Combined Genomic and IHC Analysis with a Description of a Distinct Rb-Proficient Subset. *Clin. Cancer Res.* **28**, 4702–4713 (2022).